Development of Precision Information Measuring System for Ultraviolet Radiation

Oleksiy ROSHCHUPKIN[1], Radislav SMID[1], Anatoliy SACHENKO[2,3], Volodymyr KOCHAN[2]

[1]*Faculty of Electrical Engineering, Czech Technical University, Prague, Czech Republic, Technicka 2, 166 27 Prague 6, Czech Republic*

[2]*Research Institute for Intelligent Computer Systems, Ternopil National Economic University, 3 Peremoga Square, Ternopil, 46020, Ukraine*

[3]*Department of Computer Science and Econometrics, Silesian University of Technology, Gliwice, 26 Roosevelta St, 41-800, Poland*

o.roshchupkin@ieee.org

***Abstract*—Results of studying the neural network method are presented to reduce the amount of calibration points for the multisensor (MS), in particular for the photodiode. This allows transmitting to the MS individual conversion function and provides the high accuracy of measurement.**

The structure of synthesized information-measuring system and its measuring channel has created for implementing of the proposed approach. A structural scheme is proposed as well for values transmitting the etalon measures to measuring systems. Its used to determine the errors of photodiodes, as those which are produced for customers. This assures the interchangeability of sensors when using the individual conversion function.

***Index Terms*—information-measuring system, multisensor, neural network, photodiode, individual conversion function, temperature dependency.**

I. Introduction

Nowadays the sensors error is still dominated among other components error of measuring channels (MC) in Information Measurement Systems [1]. So without reducing the sensor error it's not advisable to improve the accuracy of other MC components. For example errors of ultraviolet radiation (UVR) sensors – the photodiodes are defined by large individual deviations of their conversion functions (CF) from nominal values and those errors are strongly dependent on the temperature coefficient of photodiode.

Besides some attempts of the correction for photodiodes CF from temperature were made [4, 20], and it was based on the temperature measurement inside of the photodiode sensor frame. However, the photodiode crystal is heated by the photodiode's measurement of UVR, so it is required to measure directly the temperature of the crystal core frame. Otherwise the error (static and dynamic) appears caused by mismatching between the core crystal temperature and the photodiode sensor temperature. The same reason leads to ineffectiveness of the thermostating methods for sensor in general.

Photodiode itself can function as a temperature sensor [21], but then it should run under no-load conditions (as opposed to the mode of photodiode short circuit under the measurement of the UVR irradiance). This requires a corresponding switching the measuring scheme between the working modes of photodiode.

Under designing the precision measuring channel of UVR irradiance, it should be counted that changing the temperature of the photodiode crystal is changing also its CF towards measuring the UVR. Therefore the photodiode sensor should be considered as the multisensor(MS) [3], in which the input variables are irradiance and temperature, and output signals are the short-circuit current and the voltage at no-load conditions.

It should be noted also the transition to the individual conversion function (ICF) requires the large amount of experimental investigations for its identification. For example according to recommendations [2, 21] for the sensors with the complicated CF, for its identification, it's necessary to get the 5..7 calibration points. In such case for photodiode - the two parameter sensor of UVR are required 7*7=49 calibration points. The laboriousness of such calibrations amount is inadmissible, so it is appropriate to use a method [3, 9] of predicting the calibration result and allowing to reduce the required number of experimental explorations.

Another problem is the interchangeability of photodiodes. Known solutions [6] limit the interaction of the photodiode with the precisely customized device exactly for this photodiode CF that provides the signal conversion of the sensor into measured values as well as its indication. It does not matter whether the sensor data processing is in analog or digital form. Therefore, the damage of the measurement device requires reconfiguration with a new photodiode sensor. This situation greatly reduces the system flexibility, its vitality and repairability and creates additional problems during intensive use.

An additional important demand for UVR measurement systems is their portability and the long battery operation time, with low power consumption requirements.

A goal of this paper is developing the information-measuring system that provides highly accurate measurements of ultraviolet radiation by using the individual conversion function of the photodiode in case of irradiance, as well as in conditions of temperature influence, and assuring the sensors interchangeability in spite of transmission to the individual conversion functions.

Digital Object Identifier 10.4316/AECE.2014.03013

II. Reducing the Number of Calibration Points

During using the method [3, 9] for identification the ICF of MS, the neural networks (NN) [18, 19, 22, 23] are used as well as involved additional information of NN character. This information is contained in calibration results of the group of the same type MS (30…50 pieces) in big amount of points, for example 49. The prediction of calibration results [15, 16] will carry out for those points, for which calibration of the given MS has not been performed. In those points, for which calibration of the given MS has not been performed, conduct the prediction of calibration result using NN which is trained to predict calibration result exactly for this point. To train each NN's are used only those calibration points of the group of the same type MS which belongs to a specific set, and are always located strictly the same way relative to the calibration point which value will predict. And the calibration results of the group of similar MS are supplied to the inputs of NN in the set order. During training [3, 9] the first inputs of NN are supplied values of the ICF of that MS which is chosen for this vector of the training as a one which ICF is predicted. Then the calibration results of the group of the same type MS are supplied to the inputs of NN in order of increasing of absolute deviations from the MS, which ICF is predicted. Each such combination ICF of the group of similar MS creates one training vector.

During the prediction of each MS calibration point, to the first inputs of NN are supplied by the calibration results in another points of the MS which ICF are predicted. Then the calibration results of the group of similar MS are supplied to the inputs of NN in the order that similar to the order in the teaching stage. Calibration results of MS with the largest deviations are discarded.

For example, we obtained the calibration results of the group of similar MS in 49 points (Fig. 1, blank ring). The MS - which ICF is defined - was calibrated in 9 points (Fig. 1, filled rings). For ICF identification of this MS at the point 33 (Fig. 1) the training set is formed and it corresponds to the straight line that is drawn through the points 11, 22, 33, 44, 55, 66, 77. Then each vector of the training set has the following structure: N_{22}^{0} , N_{44}^{0} , N_{66}^{0} , N_{11}^{+1} , N_{22}^{+1} , N_{33}^{+1} , N_{44}^{+1} , N_{55}^{+1} , N_{66}^{+1} , N_{77}^{+1} , N_{11}^{-1} , N_{22}^{-1} , N_{33}^{-1} , N_{44}^{-1} , N_{55}^{-1} , N_{66}^{-1} , N_{77}^{-1} , N_{11}^{+2} , N_{22}^{+2} , … , N_{11}^{-2} , N_{22}^{-2} , … , N_{11}^{+n} , N_{22}^{+n} , … , N_{11}^{-n} , N_{22}^{-n} , … , N_{66}^{-n} , N_{77}^{-n} , where the lower indexes indicate the calibration points. The upper indexes increase with the raising of the absolute difference between the MS calibration results with index 0 (accepted for the given vector as one which ICF is predicted). The signs "+" and "-" indicate the polarity of the difference.

During the prediction as N_{22}^{0}, N_{44}^{0}, N_{66}^{0} are substituted by calibration results of the MS which ICF is identified. As it can be seen from the Fig. 1 a number of calibration points is reduced from 49 points to 9 points.

For further investigating the error of ICF identification method its nominal CF is described by the product of polynomials [5]:

$$Y_{NOM} = (A \times (X_1 + B)^k + C \times (X_1 + B)) \times \\ \times (D \times (X_2 + E)^l + F \times (X_2 + E)) \times G \quad (1)$$

where X_1, X_2 – measurable physical quantities A and B, respectively; $A…G$, k, l - coefficients and a power of number respectively; Y_{NOM} - the MS nominal output .

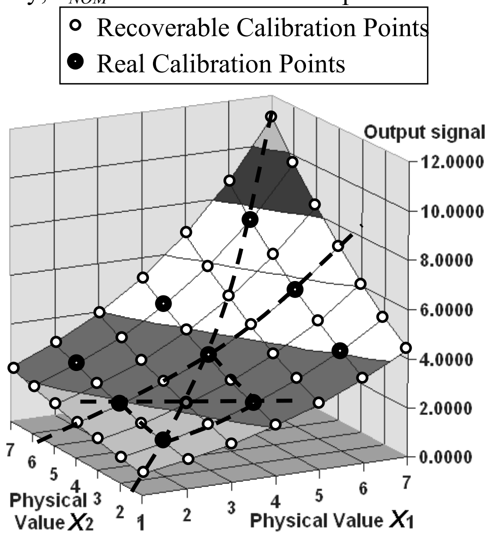

Figure 1. ICF of MS and placement of real calibration points and recoverable calibration points.

Obviously, the additive and multiplicative errors of MS can be corrected without using the NN. It's necessary therefore, to study the influence of the MS errors nonlinear component on the correction result. The MS errors of different physical quantities can be differ not only quantitatively but qualitatively too. Therefore we are exploring various combinations of the errors model described by function

$$Y = Y_{NOM} \pm n\Delta\left(\pm K_1 (i-4)^a \pm K_2 (j-4)^b\right), \quad (2)$$

where n - number of variants of the research, it was taken n = 100 (i.e. 50 experiments for each polarity); Δ – the quantization step of the error of MS, taken 0.1% (i.e. maximum error MS for each physical quantity gives 5%); K_1, K_2 - coefficients that characterize the nonlinearity of MS error function, they equal to 1%; exponents a and b can take the values 2, 3, 4 and higher orders.

Furthermore the output signal of MS is distorted by random error (random noise) which is described by function

$$Y_N = Y + Rnd\left(K_3\right), \quad (3)$$

where K_3 - coefficient, which determines the amplitude of the random error.

The Table 1 is shown the research results of prediction error of UVR MS calibration results in point 14 (Fig. 1), with different combinations of non-linear errors for both physical values. The nature of the nonlinearity of the coefficients K_1 and K_2 is shown by signs and exponents of the polynomials. The table is obtained under influence of noise with 0.1%. In the numerator shown the maximum value of the prediction error of calibration results, and in the denominator is shown mean value of the error for 100 realizations. The Table 2 is shown the research results of forecast error of UVR MS calibration results in point 34 (Fig. 1). Table 2 is obtained similarly to Table 1. However, Tables 1 and 2 describe two versions of error prediction of calibration results - interpolation (Table 1, point 14) and extrapolation (Table 2, point 34). The rest of the points should not have a fundamental difference of explored points 14 and 34, because they are located symmetrically on the MS CF. The results of additional researches confirmed the absence of a fundamental difference in the nature of error of prediction of calibration results for the other points.

TABLE 1. RESULTS OF MAXIMUM / AVERAGE PREDICTION ERRORS FOR POINT 14

PV X_1 / PV X_2	$K_1 \to +$, $k=2$	$K_1 \to -$, $k=2$	$K_1 \to +$, $k=3$	$K_1 \to -$, $k=3$	$K_1 \to +$, $k=4$	$K_1 \to -$, $k=4$
$K_2 \to +$, $k=2$	0.107 % / 0.032 %	0.134 % / 0.020 %	0.008 % / 0.002 %	0.041 % / 0.002 %	0.019 % / 0.005 %	0.030 % / 0.003 %
$K_2 \to -$, $k=2$	0.098 % / 0.030 %	0.074 % / 0.027 %	0.019 % / 0.007 %	0.033 % / 0.008 %	0.056 % / 0.009 %	0.019 % / 0.006 %
$K_2 \to +$, $k=3$	0.008 % / 0.002 %	0.041 % / 0.002 %	0.019 % / 0.005 %	0.030 % / 0.003 %	-	-
$K_2 \to -$, $k=3$	0.019 % / 0.007 %	0.033 % / 0.008 %	0.056 % / 0.009 %	0.019 % / 0.006 %	-	-
$K_2 \to +$, $k=4$	0.019 % / 0.005 %	0.030 % / 0.003 %	-	-	-	-
$K_2 \to -$, $k=4$	0.056 % / 0.009 %	0.019 % / 0.006 %	-	-	-	-

It should be noted that the maximum error value significantly (typically an order of magnitude more in) than the mean value. This means that after conducting appropriate analysis of NN's training results, user can select the best one.

TABLE 2. RESULTS OF MAXIMUM / AVERAGE PREDICTION ERRORS FOR POINT FOR POINT 34

PV X_1 / PV X_2	$K_1 \to +$, $k=2$	$K_1 \to -$, $k=2$	$K_1 \to +$, $k=3$	$K_1 \to -$, $k=3$	$K_1 \to +$, $k=4$	$K_1 \to -$, $k=4$
$K_2 \to +$, $k=2$	0.011 % / 0.004 %	0.011 % / 0.005 %	0.018 % / 0.002 %	0.023 % / 0.003 %	0.017 % / 0.004 %	0.038 % / 0.006 %
$K_2 \to -$, $k=2$	0.016 % / 0.006 %	0.005 % / 0.002 %	0.029 % / 0.016 %	0.010 % / 0.004 %	0.017 % / 0.008 %	0.186 % / 0.006 %
$K_2 \to +$, $k=3$	0.018 % / 0.002 %	0.023 % / 0.003 %	0.020 % / 0.008 %	0.022 % / 0.009 %	-	-
$K_2 \to -$, $k=3$	0.029 % / 0.016 %	0.010 % / 0.004 %	0.027 % / 0.003 %	0.049 % / 0.004 %	-	-
$K_2 \to +$, $k=4$	0.017 % / 0.004 %	0.038 % / 0.006 %	-	-	-	-
$K_2 \to -$, $k=4$	0.017 % / 0.008 %	0.186 % / 0.006 %	-	-	-	-

Figure 2 and Figure 3 are shown a dependency histograms of mean error prediction of calibration results from the nature of nonlinearity both physical values and random error during measuring for recoverable points 14 and 34.

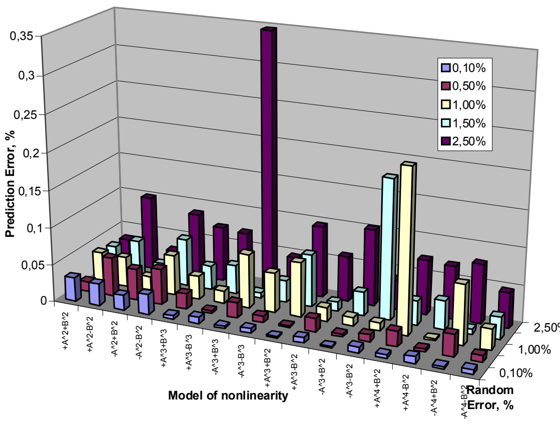

Figure 2. Dependency histogram of mean error prediction of calibration results from the nonlinearity of two physical values and value of random error for recoverable point 14

The presence of relatively large maximum errors is explained by the three-layered perceptron learning problem as the initial value of weighting coefficients are assigned randomly.

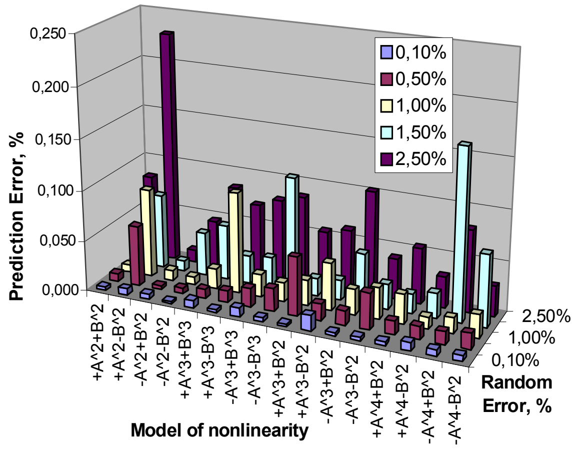

Figure 3. Dependency histogram of mean error prediction of calibration results from the nonlinearity of two physical values and value of random error for recoverable point 34

III. PROCESSING OF EXPERIMENTAL DATA

To define the photodiode ICF it is necessary to find out up to the 9 actual values of the CF photodiode deviations from the nominal one [9] for the following items:

a. the voltage drop across the photodiode on its temperature and current flowing through it;

b. short-circuit current of the photodiode on its temperature and UVR.

On the results of these experiments according to [3, 9] should be trained two NN:

1) the first NN will determine the temperature of the photodiode from voltage drop on it and current through it;

2) the second NN will determine the level of UVR on photodiode short circuit current and temperature of photodiode.

For that, during the NN training it is necessary to exchange results positions of the experiments according to items "a" and "b", that during training to the input of each NN are feed the data that defined in items 1 and 2 as the input data, and to the output of each NN are fed the data, intended for comparison, defined in items 1 and 2 as the output data.

IV. SYNTHESISS OF THE MEASURING SYSTEM STRUCTURE

Posing a task of developing the measuring system of UVR and based on the proposed approach above the following functions should be formed:

1. Setting the appropriate current across the photodiode to measure its core temperature.
2. Measuring (if necessary) a current stated in point 1above.
3. Measuring the voltage drop across the photodiode.
4. Calculating the photodiode core temperature according to measured results in points 2 and 3 above.
5. Switching the scheme in such way, to provide functioning the photodiode in short circuit mode.
6. Measuring the short circuit current of photodiode.
7. Calculating the photodiode irradiance based on results

in points 6 and 4 above.

8. Submit periodically the measured results on the display.

According to listed functions above the developing system must include the following units:

1. The photodiode – sensor of UVR.
2. The measuring channel to provide all working sensor modes.
3. Analog to digital converter (ADC).
4. Microcontroller (MC) to provide current calculations of measured results and manage the ADC and other actions of the system.
5. Digital LCD display.
6. Buttons for system operation.
7. Power source (battery - 6F22 or rechargeable battery).
8. Voltage stabilizer to eliminate the impact of battery discharging on measured results.

Based on formed functions and listed units above, we can synthesize the structure of the measuring system (Fig. 4). As its core it is profitably to use microconverter ADuC-834 [8] produced by Analog Devices, which includes the 24-bit multichannel sigma-delta ADC and microcontroller MCS-51.

The Sensor Unit consists of the UVR sensor - UV diode and electronic passport (Transducer Electronic Data Sheet, TEDS [7, 11]) that meets the requirements of the IEEE - 1451 standard. In the user part (128 bytes) of the passport are recorded the NN weights and its biases [12 - 14], [17], which are trained by the results of experimental studies of the photodiode CF according to proposed in section #2 method. This provides the transition to sensor's ICF. Interface 1-Wire have a relatively low speed, so it is no necessary to read each time all NN information which is stored in the TEDS. It is sufficiently, during each measurement to control the sensor number recorded in the standard part of TEDS [24, 25] and to read the NN data only after the sensor is replaced.

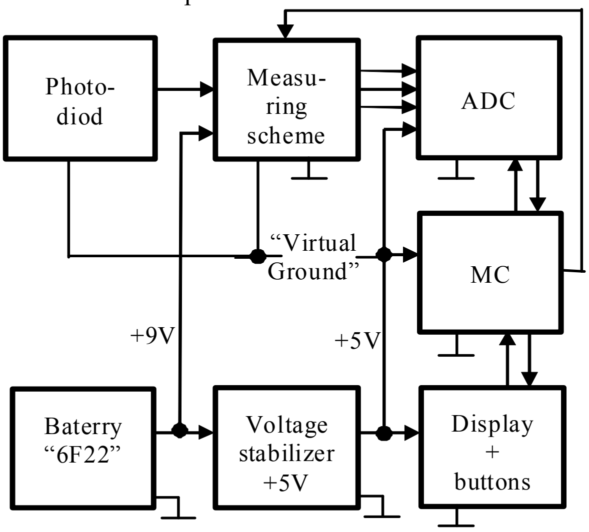

Figure 4. The structure of the measuring system.

Most complicated component part on Fig. 4 is an measuring scheme, it refers to a number of requirements during working in different modes. In particular, the short circuit mode of the photodiode with the smallest input impedance can be realized only through an operational amplifier that requires of dual polarity power supply. For this purpose into the generalized structure in Fig. 4 inserted a stabilizer, which not only eliminates the influence of low battery power during measurement results, but also creates "virtual ground" for the photodiode and operational amplifier.

V. Synthesis of the Measuring Channels

The schematic diagram of measuring channel is shown in Fig. 5. It contains photodiode FD1, semiconductor diode VD1, two operational amplifiers DA1 and DA2, resistors R1-R8, capacitors C1-C3 (filters of high frequency noise) and switch S1 (changing the mode of operation: the metering of the UVR or temperature monitoring).

The UVR measuring channel forms the mode of short circuit for photodiode FD1 and includes operational amplifier DA2, that operates in inverter mode [10], resistor R2 used as a feedback, and has the voltage divider (resistors R4 and R8) for correlation of signal levels that entering the output U_{V1} of the ADC and its supply voltage. When switch S1 is in left position (the mode of short circuit for photodiode FD1) voltage of the output DA2 is lower than the voltage of "virtual ground" U_{z1}, so diode VD1 is locked and R1 is not affected on functioning of DA2.

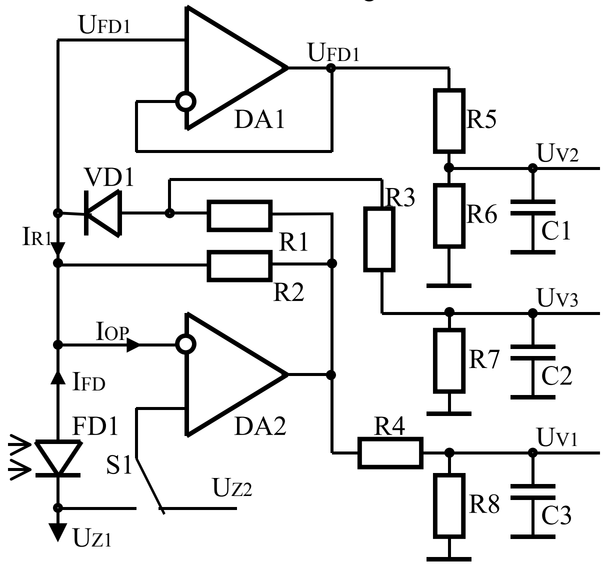

Figure 5. Schematic diagram of the measuring channels for ultraviolet radiation

Based on the ADC results of voltage U_{V1} conversion, the current I_{PD1}^{SS} of photodiode PD1 can be determined from the formula

$$\frac{I_{PD1}^{SS} \cdot R2 \cdot R8}{R4 + R8} = U_{V1} \tag{4}$$

By transforming (4), we obtain

$$I_{PD1}^{SS} = \frac{U_{V1} \cdot (R4 + R8)}{R2 \cdot R8}. \tag{5}$$

The temperature measuring channel (photodiode PD1 is at idle in this mode) contains an operational amplifier DA1 (operating in non-inverting mode) and its large input impedance prevents PD1 from the load by divider R5, R6. In the measurement of temperature S1 is in the right position so the voltage U_{z1} on the DA2 input exceeds voltage of U_{z2} and DA2 is saturated - its output voltage approaches to the supply voltage of 9V. Then VD1 is opened, current I_{R1} of resistor R1 also flows through PD1. The current I_{PD1} will

$$I_{PD1} = I_{R1} + I_{R2}\,. \tag{6}$$

In turn,

$$I_{R1} = (U_{DA2}^{SAT} - U_{PD1} - U_{VD1}) / R1 \tag{7}$$

$$I_{R2} = (U_{DA2}^{SAT} - U_{PD1}) / R2 \tag{8}$$

where U_{DA2}^{SAT} - the operating voltage saturation of the DA2 operation amplifier, $U_{DA2}^{SAT} \approx U_{Z2} = 9V$; U_{VD1} - voltage drop across the diode VD1 in the conducting state, $U_{VD1} \approx 0{,}7V$.

It should be noted that the values of the voltage U_{DA2}^{SAT} and the U_{VD1} voltage value, firstly - is known approximately and secondly - they have significant temperature fluctuation. That is why we need to define the values I_{R1}, I_{R2} during the operation of UVR measuring system. To define I_{R2} we can use U_{V1} and U_{V2}. According to Fig. 5 can be written

$$U_{V1} = U_{DA2}^{SAT} \frac{R8}{R4 + R8} \tag{9}$$

$$U_{V2} = U_{PD1} \frac{R6}{R5 + R6}\,. \tag{10}$$

By transforming (9) and (10) and substituting it in (8), we obtain

$$I_{R2} = (U_{V1} \frac{R4 + R8}{R8} - U_{V2} \frac{R5 + R6}{R6}) / R2\,. \tag{11}$$

In (7) the U_{VD1} is also unknown. Therefore, to define I_{R1} lets create the measuring channel, formed by divider R3 and R7. The voltage on the left pin of R1 can be defined as the summing of "virtual ground" voltage U_{z1}, voltage drop on photodiode U_{PD1} and the voltage drop U_{VD1} on diode. This voltage will be higher than U_{z1} "virtual ground" voltage, that is higher than the ADC conversion ranges (ADC is powered from U_{Z1}). Therefore divider of R3 and R7 matches voltage on left pin of R1 with acceptable voltage U_{V3}. Then the voltage on $R1$ can be determined as how

$$U_{R1} = U_{V1} \frac{R4 + R8}{R8} - U_{V3} \frac{R3 + R7}{R7}\,. \tag{12}$$

Hence the current I_{R1} is

$$I_{R1} = \frac{1}{R1}\left(U_{V1} \frac{R4 + R8}{R8} - U_{V3} \frac{R3 + R7}{R7} \right). \tag{13}$$

VI. WAYS OF ASSURING THE SENSORS INTERCHANGEABILITY

A ttransition to the photodiode ICF allows to reduce an effect of the its CF dispersion on the measurement result. But values of resistances R1-R8 (their deviation from the nominal value) also affect the voltage $U_{V1}...U_{V3}$. To assure the sensors interchangeability authors proposed the following two ways. According to the first one measuring channels are included into sensor itself (Fig.4). Then, while a determination of the photodiode ICF is deteminating the experimental studies are running along with measurement channels where the photodiode FD1 is operating. Values of resistors R1-R8 will be count in the calibration results, and the error of the UV measurement will be defined only by temperature and temporal changes of those resistors resistance. If there are used inaccurate (with the large acceptable deviations of the real resistance from the nominal value), but stable resistors (e.g. metal-film resistor), then it's possible to obtain the precision result of measurements at low costs. However, this method requires equipping each sensor by measuring channels that is economically unreasonable.

The second way of assuring the sensors interchangeability is delimiting the corrections of the sensor and the measuring channel. In this case, each sensor is equipped with TEDS [7], in which weights of neurons and its bias are recorded only for NN of errors correction of this sensor without taking into account of measuring circuit.

Moreover each UVR measuring system is equipped by its own TEDS of measurement system error correction and ADC (the source of its reference voltage). In this case the commercial(produced) system and the system for sensors research(while identifying its ICF), have a similar scheme. So it's possible to run the process of identifying and correcting errors of all components in such a way when its errors are mutually compensated.

The Fig. 6 illustrates the process of errors determination and correction using the second method of the UVR sensors interchangeability. Firstly, using standard measurement tools (or assignment) of the voltage *U* should be calculated the errors of measurement voltage drop channels on the photodiode for the commercial(produced) systems and the system for sensors research. Calculation of correcting coefficients is performed by personal computer (PC) and it records those results in TEDS-E of the appropriate systems.

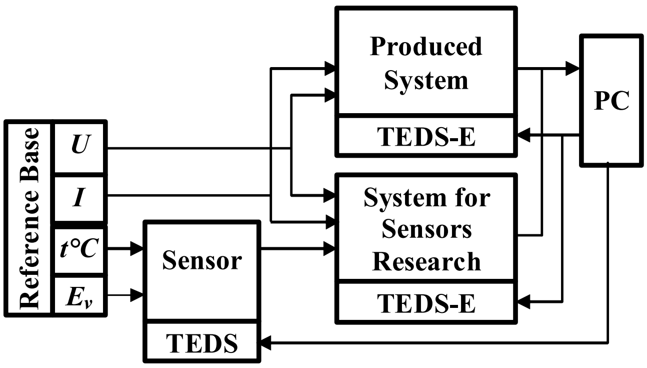

Figure 6. Scheme of process for error determination and correction

Similarly, the correcting coefficients can be determined and recorded in the TEDS-E appropriate cells of all systems for channels of the photodiode current during the temperature measurement as well as short circuit current. For this purpose, besides to reference tools of the measuring voltage *U*, a precision tool for the current measurement *I* is used. As a result, all systems will have the identical CF of photodiodes for all channels. Differences between their CF will be determined by their random error only. In this case, the weights and bias of the NN, which corresponds to the ICF per each studied photodiode, will be defined in identical conditions.

Experimental researches confirmed the non-exceptional errors of measuring channels are determined (if errors of reference instruments are discounted), by its noises and short-term instability only.

VII. Conclusions

The article reflects the results of studying the neural network method to reduce the multisensor calibration points, in particular for the photodiode, which is considered as the multisensor. This enables an efficient transition to the individual conversion function of photodiode and ensures a correction of errors caused by the dominant influencing quantity - the temperature of the photodiode crystal. It's proposed also a sequence of processing the measurement results at the transition to the individual conversion function.

Based on proposed approach a generalized structure of information-measuring system and the precision measuring channel both are synthesized. Moreover a way to assure sensors interchangeability at the use of the individual conversion function, and a corresponding scheme of process for error determination and correction were designed.

The proposed solutions can be considered as a base for the creating the precision information-measuring systems for the irradiance of ultraviolet radiation.

References

[1] A. A. Sachenko. Designing of Intelligent Measuring Systems of Nonelectric Quantities. Engineering Systems with Intelligence, Microprocessor-Based and Intelligent Systems Engineering, Vol. 9, pp 679-686, 1991. [Online]. Available: http://dx.doi.org/10.1007/978-94-011-2560-4_78

[2] Manual on the use of Thermocouples in Temperature Measurement. ASTM Committee E20 on Temperature Measurement - 4th ed. - Philadelphia, ASTM, 1993. - 290p. ISBN: 0-8031-1466-4

[3] Roshchupkin O., Smid R., Kochan V., Sachenko A. Reducing the Calibration Points of Multisensors. Proceedings of the 9th IEEE International Multi-Conference on Systems, Signals and Devices (SSD'2012). - Chemnitz ,Germany, March 20 - 23, 2012. Pp.1-6. [Online]. Available: http://dx.doi.org/10.1109/SSD.2012.6197987

[4] ST120 Dual Silicon Based Thermopile Detector: 2 Channels. [Online]. Available: http://www.dexterresearch.com/?module=Page &sID=st120-dual

[5] Turchenko I. Accurate Recognition of Multi-Sensor Output Signal Using Modular Neural Networks / Turchenko I., Kochan V., Sachenko A. // International Journal of Information Technology and Intelligent Computing. – 2007. – Vol. 2, No. 1. – P. 27- 47.

[6] Butenko V.K. Radiometer of ultraviolet radiation - "Tensor-31" / V.K. Butenko, V.G. Yurev // TKEA. 2006. Vol. 6. Pp. 36-38. (In Russian)

[7] Song, Eugene Y., and Kang Lee. "Understanding IEEE 1451-Networked smart transducer interface standard-What is a smart transducer?" Instrumentation & Measurement Magazine, IEEE 11.2 (2008): 11-17. [Online]. Available: http://dx.doi.org/10.1109/ MIM.2008.4483728

[8] ADUC845: Precision Analog Microcontroller. [Online]. Available: http://www.analog.com/ru/processors-dsp/analog-microcontrollers/ aduc845 /products/product.html

[9] Patent of Ukraine for Inventions # 103802 registered on 25.11.2013. Application # a2011 13840, declared 24.11.2011. Method of Multisensor Convertion Function Identification. Roshchupkin O. U., Kochan V. V., Sachenko A. O. (In Ukrainian) [Online]. Available: http://library.ukrpatent.org/document?fund=1&id=194048&to_fund=1

[10] G. B. Clayton, S. Winder. Operational amplifiers. Elsevier, 2003. ISBN: 978-0-7506-5914-7

[11] D. Wobschall A Multi-port Serial NCAP using IEEE1451 Smart Transducer Standard / D. Wobschall, A. Stepanenko, I. Maykiv, R. Kochan, A. Sachenko, V. Kochan // IEEE Sensor Application Symposium (SAS-2009): IEEE international conference, 17-19 February 2009: proceedings. - New Orleans, USA, 2009. - P.293-297. [Online]. Available: http://dx.doi.org/10.1109/SAS.2009.4801818

[12] J. Rivera-Mejia, M. Carrillo-Romero, G. Herrera-Ruiz. Self-compensation to build reconfigurable measurement systems. Instrumentation & Measurement Magazine, IEEE (Volume:16 , Issue: 2). 2013. Pp. 10 – 19 [Online]. Available: 10.1109/ MIM.2013.6495675

[13] J. N. Cotton, M. B. Wilamowski, "Compensation of Sensors Nonlinearity with Neural Networks" // Proceedings of the 2010 24th IEEE International Conference on Advanced Information Networking and Applications pp. 1210-1217. 2010. [Online]. Available: http://www.eng.auburn.edu/~wilambm/pap/2010/Compensation%20of%20Sensors%20Nonlinearity%20with.pdf

[14] Yu Hen Hu, Jenq-Neng Nwang. "Handbook of Neural Network Signal Processing." – CRC Press, 2002. p. 408. ISBN 0-8493-2359-2

[15] M. J. Rivera, R. M. Carrillo, M. M. Chacon, R. G. Herrera, D. G. Bojorquez, "Self-calibration and optimal response in intelligent sensors design based on artificial neural networks," Sensors, vol. 7, pp. 1509-1529, Aug. 2008, ISSN 1424-8220. [Online]. Available: http://www.mdpi.com/1424-8220/7/8/1509/pdf

[16] D.E. Rumelhart, G.E. Hinton, R.J. Williams "Learning internal representations by error propagation". // Parallel Distributed Processing, Vol. I Foundations. - MIT Press, Cambridge, MA, 1986., – pp. 315 – 328. ISSN: 00280836 [Online]. Available: http://psych. stanford.edu/~jlm/papers/PDP/Volume%201/Chap8_PDP86.pdf

[17] Oleksiy Roshchupkin, Radislav Smid, Volodymyr Kochan, Anatoly Sachenko. Multisensors Signal Processing Using Microcontroller and Neural Networks Identification. Sensors & Transducers Journal, Vol.24, No.8, 2013, pp. 1-6. [Online]. Available: http://www. sensorsportal.com/HTML/DIGEST/P_SI_425.htm

[18] Michie D., Spiegelhalter D.J., Taylor C.C. Machine Training, Neural and Statistical Classification / New York: Ellis Horwood, 1994. 290 p. [Online]. Available: http://www1.maths.leeds.ac.uk/~charles /statlog/

[19] H. Zhang, M. Balaban, J. Principe, "Improving pattern recognition of electronic nose data with time-delay neural networks", Sensors and Actuators B, Vol. 96, No. 1-2, 2003, pp. 385-389. [Online]. Available: doi:10.1016/S0925-4005(03)00574-4

[20] Si photodiode S2592/S3477 series - Hamamatsu. [Online]. Available: http://www.hamamatsu.com/resources/pdf/ssd/s2592-03_etc_kspd1003e07.pdf

[21] Fraden J. Handbook of Modern Sensors: Physics, Designs, and Applications, Springer, 2010, 663p. [Online]. Available: DOI 10.1007/978-1-4419-6466-3

[22] Kroese B. An introduction to Neural Networks. Amsterdam: University of Amsterdam, 1996, 120p. [Online]. Available: http://lia.univ-avignon.fr/chercheurs/torres/livres/book-neuro-intro.pdf

[23] Haykin S. Neural networks. Macmillan College Publishing Company, Inc., New York, 1994. ISBN 0-02-352761-7, 696p.

[24] E. Brignell, "Digital compensation of sensors", Scientific Instruments. Vol. 20, N 9, 1987, pp. 1097-1102. [Online]. Available: DOI: 10.1088/0022-3735/20/9/005

[25] Taner A., Brignell J. Virtual instrumentation and intelligent sensors, Sensors and Actuators A: Physical, Vol. 61, No. 1-3. 1997, pp. 427-430. [Online]. Available: http://dx.doi.org/10.1016/S0924-4247(97)80300-7